

Real-Time Coordination of Plug-In Electric Vehicle Charging in Smart Grids to Minimize Power Losses and Improve Voltage Profile

Sara Deilami, *Student Member, IEEE*, Amir S. Masoum, *Student Member, IEEE*,
Paul S. Moses, *Student Member, IEEE*, and Mohammad A. S. Masoum, *Senior Member, IEEE*

Abstract—This paper proposes a novel load management solution for coordinating the charging of multiple plug-in electric vehicles (PEVs) in a smart grid system. Utilities are becoming concerned about the potential stresses, performance degradations and overloads that may occur in distribution systems with multiple domestic PEV charging activities. Uncontrolled and random PEV charging can cause increased power losses, overloads and voltage fluctuations, which are all detrimental to the reliability and security of newly developing smart grids. Therefore, a real-time smart load management (RT-SLM) control strategy is proposed and developed for the coordination of PEV charging based on real-time (e.g., every 5 min) minimization of total cost of generating the energy plus the associated grid energy losses. The approach reduces generation cost by incorporating time-varying market energy prices and PEV owner preferred charging time zones based on priority selection. The RT-SLM algorithm appropriately considers random plug-in of PEVs and utilizes the maximum sensitivities selection (MSS) optimization. This approach enables PEVs to begin charging as soon as possible considering priority-charging time zones while complying with network operation criteria (such as losses, generation limits, and voltage profile). Simulation results are presented to demonstrate the performance of SLM for the modified IEEE 23 kV distribution system connected to several low voltage residential networks populated with PEVs.

Index Terms—Generation cost, hourly prices and smart grid, load management, plug-in electric vehicles, real time.

I. INTRODUCTION

PLUG-IN electric vehicles (PEVs) are growing in popularity as more efficient low emission alternatives to the conventional fuel-based automobiles. Depleting natural oil and fossil fuel reserves, rising petrol costs, and increasing governmental regulations to adopt more sustainable technologies have driven the development of plug-in electric vehicles. Nissan, Mitsubishi, General Motors, and Chevrolet [1]–[3] have already begun to roll out PEVs from their production lines with many more automotive companies promising to rapidly expand into the PEV market.

The operation of PEVs in a distribution system will be a challenging demand side management (DSM [4], [5]) problem from the utilities perspectives since PEV battery chargers represent sizeable loads. A quite plausible scenario is that numerous PEV owners will arrive home from work within a narrow time

Manuscript received August 18, 2010; revised December 24, 2010; accepted May 29, 2011. Date of current version August 24, 2011. Paper no. TSG-00112-2010.

The authors are with the Department of Electrical and Computer Engineering, Curtin University, Perth, WA, 6845, Australia (e-mail: s.deilami@postgrad.curtin.edu.au; a_masoum@ieec.org; paul.s.moses@gmail.com; m.masoum@curtin.edu.au).

Color versions of one or more of the figures in this paper are available online at <http://ieeexplore.ieee.org>.

Digital Object Identifier 10.1109/TSG.2011.2159816

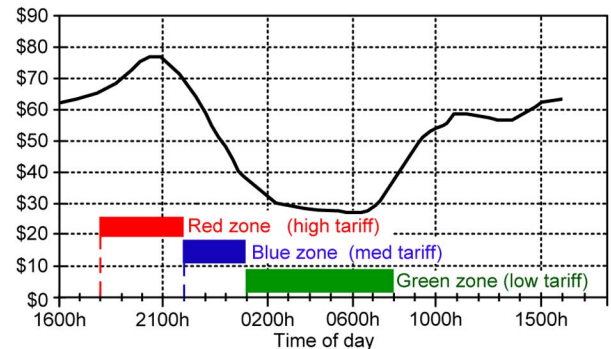


Fig. 1. Subscription options of charging time zones for PEV owners and variable short-term market energy pricing [30].

period and immediately plug-in their vehicles to charge during a time of already high peak demand. These uncoordinated and random charging activities could significantly stress the distribution system causing severe voltage fluctuations, sub-optimal generation dispatch, degraded system efficiency and economy, as well as increasing the likelihood of blackouts due to network overloads. Fortunately, the development of smart grid communication infrastructure will provide an excellent opportunity to manage this problem with intelligent or smart coordinated charging of PEVs.

Smart grid technologies are currently undergoing development in an effort to modernize legacy power grids to cope with increasing energy demands of the future [6]–[8]. Although the details and standards for smart grids have yet to be finalized, it is clear that a high speed bidirectional communications network will be necessary. This will provide the framework for real-time monitoring and control of transmission, distribution, and end-user consumer assets for effective coordination and usage of available energy resources.

Some recent publications have studied the integration of customer DSM for demand response and load control in smart grids to improve the system load profile and reduce peak demand [9]–[13]. To achieve this, many countries are developing technologies such as smart metering and smart appliances. Italy and Sweden, for example, are approaching 100% deployment of smart meters for consumers. Smart appliances such as PEVs will soon be able to “talk” to the grid and exercise a more advanced form of (semi)automated DSM by automatically scheduling their activities at strategic times [14]–[16]. Electric vehicles can also be utilized to support smart grids by offering ancillary services such as frequency regulation [24]–[26] and energy storage. Reference [24] uses dynamic programming to make efficient use of the distributed power of electric vehicles

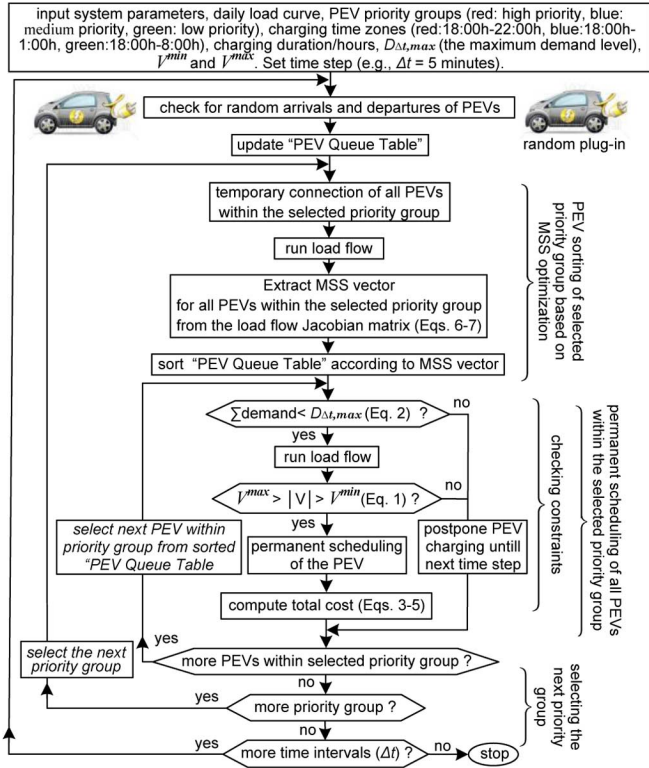


Fig. 2. Proposed MSS-based RT-SLM algorithm for coordinated PEV scheduling with random arrivals and departures of PEVs at each time step (e.g., $\Delta t = 5$ min) considering system losses, voltage profile, and peak demand limits.

and develops an optimal vehicle-to-grid (V2G) aggregator for frequency regulation. It focuses on the individual PEV charging scheduling rather than collectively organizing the PEVs as proposed in this paper. These expanding functionalities enables smart grids to rapidly self-regulate and heal, improve system reliability and security, and more efficiently manage energy delivery and consumption [17]–[23].

In support of these objectives, this paper proposes a novel real-time smart load management (RT-SLM) algorithm to coordinate multiple PEV charging activities while reducing system stresses that can impact grid reliability, security and performance [17]. The proposed sensitivities-based RT-SLM allocates PEVs for charging as soon as possible based on real-time (e.g., every 5 min) cost minimization and improves voltage profile while considering designated charging time zone priorities specified by PEV owners. To demonstrate the improvements in smart grid performance, RT-SLM is simulated with a detailed system topology consisting of a high voltage (HV) feeder with several integrated low voltage (LV) residential networks populated with PEVs. Simulation results are presented for (un)coordinated charging with PEV penetrations of 16%, 32%, 47%, and 63% considering three designated time zones; red: 1800h-2200h, blue: 2200h-0100h, and green: 0100h-0800h.

II. PEV CHARGING COORDINATION: PROBLEM FORMULATION

The PEV charging coordination problem is formulated into a series of system constraints and an objective function necessary to improve smart grid performance and economy.

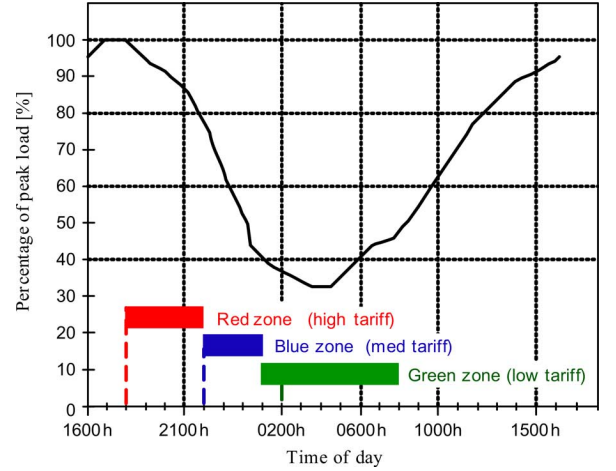


Fig. 3. Daily residential load curve.

TABLE II
PEV CHARGING SCENARIOS FOR SMART GRID SYSTEM OF FIG. 4 WITH PEV CHARGING TIME ZONES AND DAILY LOAD CURVE OF FIG. 3

| Case | Charging Scheme ($\Delta t = 5$ minutes) |
|------|---|
| A | Uncoordinated random charging over 1800h-0800h (Case A1), 1800h-0100h (Case A2) and 1800h-2200h (Case A3). |
| B | Coordinated RT-SLM charging with a constant maximum demand level of $D_{\Delta t, \max} = 0.84$ MW considering consumer priorities while intentionally allowing the medium and low priority consumers to charge their PEVs at earlier hours if there is enough capacity. |
| C | Coordinated RT-SLM charging with a constant maximum demand level of $D_{\Delta t, \max} = 0.84$ MW while preventing the medium and low priority consumers to charge at earlier hours (e.g., red, blue and green consumers can only begin charging their PEVs at 1800h, 2200h, and 0100h, respectively). |
| D | Same as Case C except with step-varied demand limits $D_{\Delta t, \max}$ of 0.84 MW, 0.70 MW and 0.60 MW in red, blue and green time zones, respectively. |

A. System Constraints

The voltage constraints of the distribution system will be considered by setting the upper and lower limits to correspond to voltage regulation limits typically set by utilities. In this paper, the voltage limits are set to $\pm 10\%$ ($V^{\min} = 0.9$ pu and $V^{\max} = 1.1$ pu) which is typical of many distribution systems

$$V^{\min} \leq V_k \leq V^{\max} \text{ for } k = 1, \dots, n. \quad (1)$$

where k and n are the node number and total number of nodes, respectively. The second constraint is for setting a ceiling limit for the total maximum system demand of the distribution system to prevent an overload condition from PEV charging

$$P_{\Delta t}^{\text{total demand}} = \sum_k P_{\Delta t, k}^{\text{load}} \leq D_{\Delta t, \max} \quad (2)$$

where $P_{\Delta t}^{\text{total demand}}$ is the total power consumption at time interval Δt within the 24 h, $P_{\Delta t, k}^{\text{load}}$ is the power consumption of node k at Δt and $D_{\Delta t, \max}$ is the maximum demand level at Δt that would normally occur without any PEVs.

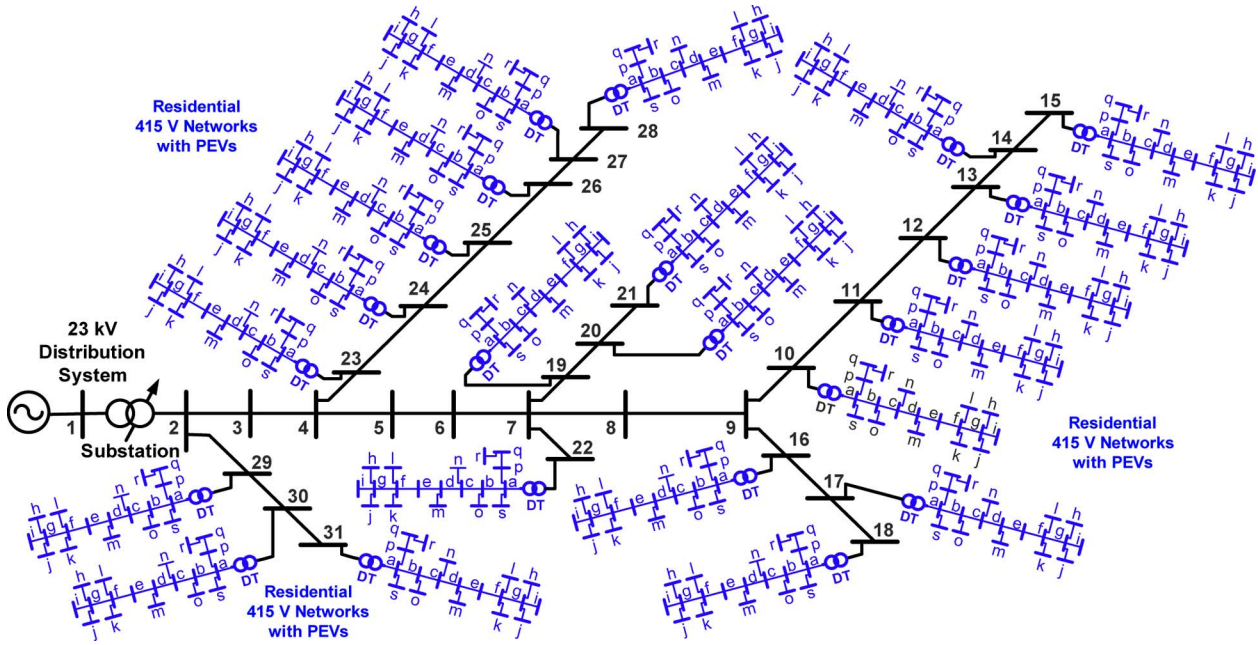


Fig. 4. The 449 node smart grid distribution system topology consisting of the IEEE 31 node 23 kV system with several 415 V residential feeders. Each LV residential feeder has 19 nodes representing customer households with varying penetrations of plug-in electric vehicles (Table I).

B. Objective Function (Cost Index)

The selected objective function for the PEV charging coordination problem is based on the minimization of total cost of purchasing or producing the energy for charging PEVs plus the associated grid energy losses. The justification for this is that the economy of smart grids will largely depend on the cost of energy that would be expended on cable and transformer losses. Therefore, the following objective function is defined:

$$\begin{aligned} \min F_{\text{cost}} &= F_{\text{cost-loss}} + F_{\text{cost-gen}} \\ &= \sum_{\Delta t} K_E P_{\Delta t}^{\text{total loss}} \\ &\quad + \sum_{\Delta t} K_{\Delta t, G} P_{\Delta t}^{\text{total demand}} \end{aligned} \quad (3)$$

where $F_{\text{cost-loss}}$ and $F_{\text{cost-gen}}$ are the costs corresponding to total system losses and total generation, respectively; Δt is the time interval (e.g., $\Delta t = 5$ min), K_E is the cost per MWh of losses (e.g., $K_E = 50$ \$/MWh, [27]–[29]) and $K_{\Delta t, G}$ is the cost per MWh of generation at time interval Δt based on the variable price of purchasing or producing the energy (e.g., Fig. 1, [30]). $P_{\Delta t}^{\text{total loss}}$ is the total power losses of distribution system for time interval Δt

$$P_{\Delta t}^{\text{total loss}} = \sum_{k=0}^{n-1} P_{\Delta t, (k, k+1)}^{\text{loss}} \quad (4)$$

$$\begin{aligned} P_{\text{loss}} &= P_{\Delta t, (k, k+1)}^{\text{loss}} \\ &= R_{k, k+1} (|V_{k+1} - V_k| |y_{k, k+1}|)^2 \end{aligned} \quad (5)$$

where V_k is the voltage at node k at time interval Δt , while $P_{\Delta t, (k, k+1)}^{\text{loss}}$, $R_{k, k+1}$ and $y_{k, k+1}$ are power loss, resistance, and admittance of line section between nodes k and $k+1$.

In this paper, optimization of $F_{\text{cost-loss}}$ and $F_{\text{cost-gen}}$ (3) are performed by minimizing system losses at each time interval Δt

TABLE I
DESIGNATED PEV PENETRATION LEVELS AND ASSIGNED PRIORITIES FOR CHARGING TIME ZONES (RED=HIGH PRIORITY, BLUE=MEDIUM PRIORITY, GREEN=LOW PRIORITY)

| 19 Node System | PEV Penetration Levels | | | |
|----------------|------------------------|-----|-----|-----|
| | 16% | 32% | 47% | 63% |
| a | | | | |
| b | | | | |
| c | | | | |
| d | | | | |
| e | | | | |
| f | | | | |
| g | | | | |
| h | | | | |
| i | | | | |
| j | | | | |
| k | | | | |
| l | | | | |
| m | | | | |
| n | | | | |
| o | | | | |
| p | | | | |
| q | | | | |
| r | | | | |
| s | | | | |

*) Boxes with no color indicate nodes with no PEVs present

and incorporating time-varying energy prices over the 24 hours and PEV owner preferred charging time zones based on priority selection.

In order to assess the state of a smart grid subject to PEV charging as well as generation status, voltage profile, and power losses necessary for the objective function and checking of constraints, a modified Newton-based load flow routine is used. All loads are modeled as constant power loads with their real and reactive powers updated through a daily load curve for each time interval the load flow is performed.

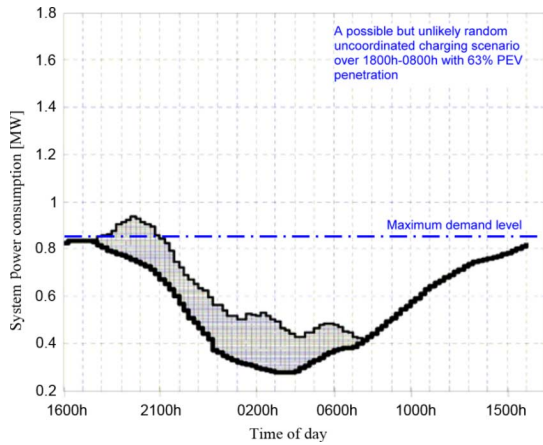


Fig. 5. Case A1: Impact of random uncoordinated PEV charging (63% penetration) within 1800h-0800h on system demand.

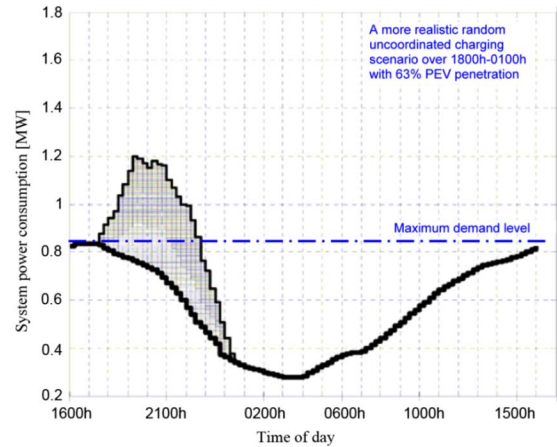


Fig. 8. Case A2: Impact of random uncoordinated PEV charging (63% penetration) within 1800h-0100h on system demand.

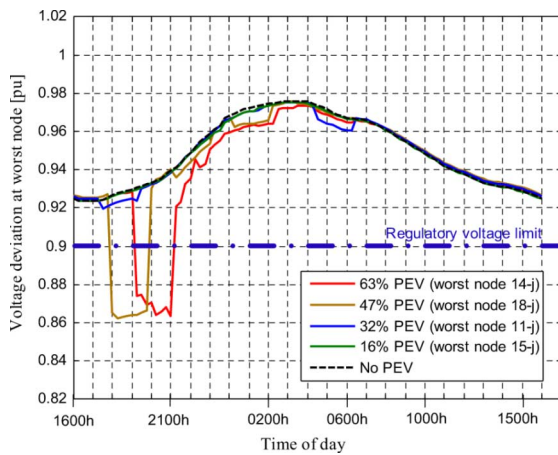


Fig. 6. Case A1: Impact of random uncoordinated PEV charging within 1800h-0800h on voltage profile (shown for worst affected nodes). High PEV penetrations cause moderate voltages deviations.

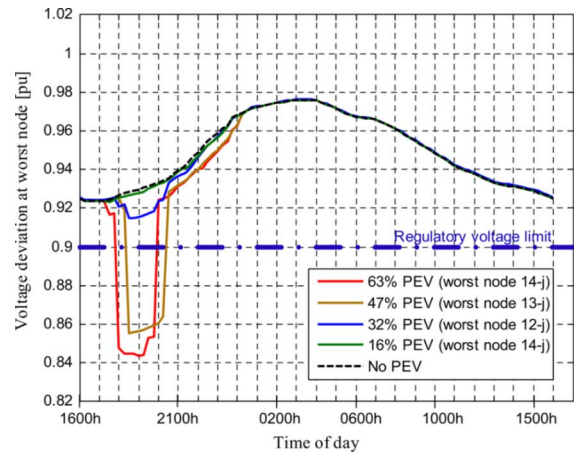


Fig. 9. Case A2: Impact of random uncoordinated PEV charging within 1800h-0100h on voltage profile (shown for worst affected nodes). High PEV penetrations cause moderate voltages deviations.

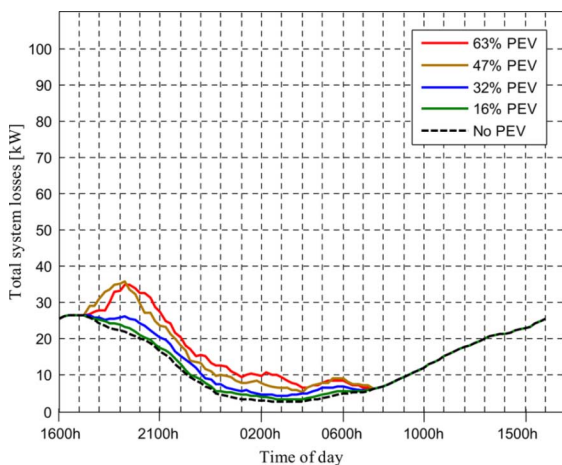


Fig. 7. Case A1: Impact of random uncoordinated PEV charging within 1800h-0800h on the total system power losses.

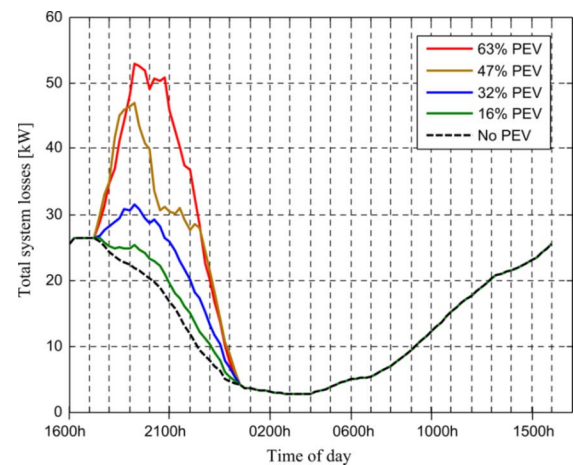


Fig. 10. Case A2: Impact of random uncoordinated PEV charging within 1800h-0100h on the total system power losses.

III. REAL-TIME SLM ALGORITHM WITH RANDOM ARRIVALS OF PEVS CONSIDERING CONSUMER PRIORITY

A new real-time smart load management (RT-SLM) approach for the coordination of PEV charging is proposed to improve

the security and reliability of smart grids by minimizing voltage deviations, overloads, and power losses that would otherwise be impaired by random uncoordinated PEV charging. The random and unpredictable nature of PEV activity in a domestic household situation calls for a fast and adaptable real-time coordination strategy.

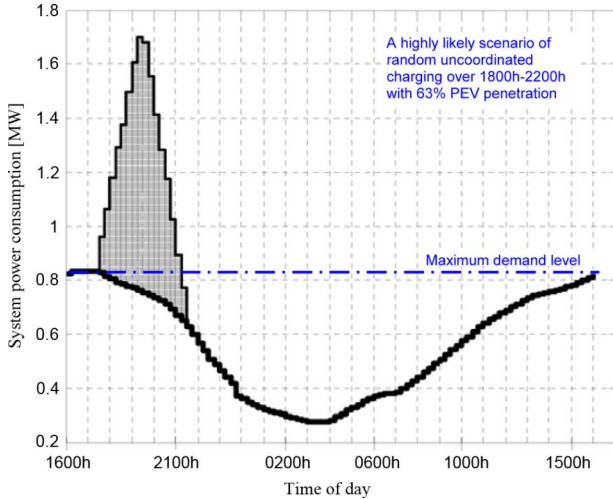


Fig. 11. Case A3: Impact of random uncoordinated PEV charging (63% penetration) within 1800h-2200h on system demand.

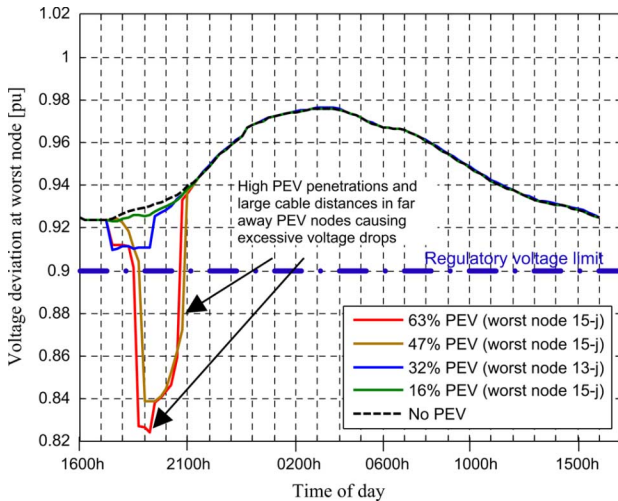


Fig. 12. Case A3: Impact of random uncoordinated PEV charging within 1800h-2200h on voltage profile (shown for worst affected nodes). High PEV penetrations result in large voltage deviations.

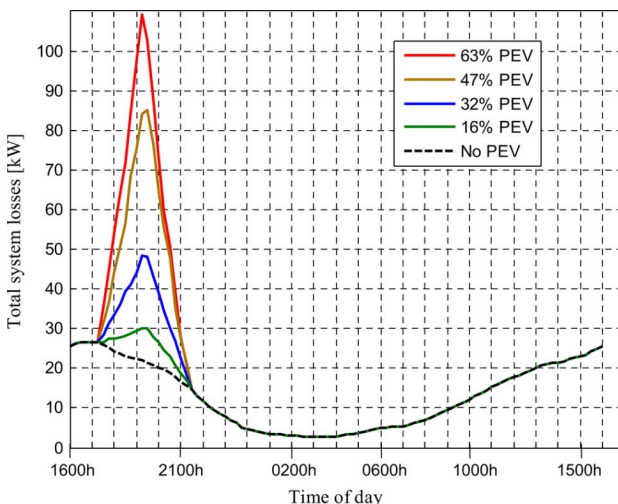


Fig. 13. Case A3: Impact of random uncoordinated PEV charging within 1800h-2200h on total system power losses.

A. Overview of RT-SLM

As an alternative to PEV chargers randomly and immediately operating when first plugged in, or after some fixed time delay, the proposed RT-SLM will decide which PEVs will charge at what time. PEV charger control can be achieved through the forthcoming smart grid communications infrastructure by sending and receiving signals to individual PEV chargers. This means that PEV charging control would be taken out of the hands of the owner and scheduled automatically. RT-SLM will perform cost minimization based on (3) and the system constraints (1)–(2). Furthermore, load variations and energy pricing over a 24 h cycle with PEV owner preferences for charging time zone and priority are included. Based on this and load flow computed outputs, RT-SLM assigns charging schedules for individual PEVs to maximize smart grid operational performance.

B. Charging Zone and Priority Scheme

The cost of purchasing or producing the energy for charging PEVs is minimized by defining time zones to correspond with utilities interest in minimizing generation during on-peak times. PEV owners will indicate their preferred charging time zone and at each time step (e.g., $\Delta t = 5$ min), RT-SLM will try to accommodate these preferences while considering the cost minimization objective function and system constraints(1)–(5). Three charging zones have been defined for this study:

- Red charging zone (1800h-2200h)- coinciding with most of the on-peak period and is designated for (high priority) PEV owners wanting to charge their PEVs as soon as possible on return from work in order to have their vehicles ready for use later in the evening. These PEV owners desiring to charge during this period of high demand will be charged a higher tariff rate.
- Blue charging zone (2200h-0100h)- is for (medium priority) consumers that prefer to charge their vehicles at partially off-peak periods and pay a lower tariff rate.
- Green charging zone (0100h-0800h)- is the period that most PEV charging will take place since most (low priority) consumers will require their vehicles fully charged for use throughout the next day. Charging off-peak will be highly encouraged by setting the cheapest tariff rates (Fig. 1).

Note that the three charging zone periods (Fig. 1) do not overlap. However, RT-SLM will also allow high and medium priority subscribers to charge their vehicles if they arrive after 2200h and 0100h, respectively. In practice, priority consumers that arrive in their preferred red and blue charging time zones and are unable to be charged due to network constraints should be compensated. This is not included in the present version of RT-SLM and will be considered in future research.

C. PEV Coordination Based on MSS Optimization

Real-time coordination of PEVs involves loss minimization ((3), $F_{\text{cost-loss}}$), voltage regulation (1) and peak demand control (2) while respecting PEV owner priorities ((3), $F_{\text{cost-gen}}$). Therefore, the inclusion of optimization techniques would seem to be in order. However, conventional optimization approaches such as genetic algorithms (GAs) are not computationally efficient for real-time applications with short time steps (e.g., 5 min). Therefore, the proposed RT-SLM employs the maximum

sensitivities selection (MSS) optimization approach to minimize system losses [27]–[29].

MSS quantifies the objective function sensitivities (system losses) to PEV charger loads in the smart grid at a given time step. This is achieved by temporarily activating in the load flow all PEV charger nodes (at 5% of their nominal power rating) in the queue at the current time step. From the small load power perturbations at each PEV charger node, it is then possible to conveniently compute the sensitivities of system losses due to each of the candidate PEV nodes from Jacobian entries of the load flow, which is then stored in the MSS vector. The MSS vector is then sorted such that PEVs contributing to the highest loss sensitivities in each priority group are selected last. In this manner, the PEV coordination solution is designed to favor scheduling first the PEVs causing minimum impact on system losses. This MSS sorting process is repeated for descending priority groups thereby arriving at a sorted PEV queue table in accordance with the MSS vector.

Sensitivities of the objective function [(3), $F_{\text{cost-loss}}$] to the PEV location and power consumption can be computed using partial derivatives [27]–[29]

$$MSS_j = \frac{\partial P_{\text{loss}}}{\partial P} \quad (6)$$

where MSS_j is the sensitivity of PEV at node j , P_{loss} is total power loss (5) and P is the power consumption of PEV. Partial derivatives of P_{loss} are deduced from the Jacobian matrix of the load flow as follows:

$$\begin{bmatrix} \frac{\partial P_{\text{loss}}}{\partial P} \\ \frac{\partial P_{\text{loss}}}{\partial Q} \end{bmatrix} = \begin{bmatrix} \frac{\partial P}{\partial \theta} & \frac{\partial Q}{\partial \theta} \\ \frac{\partial P}{\partial |V|} & \frac{\partial Q}{\partial |V|} \end{bmatrix}^{-1} \begin{bmatrix} \frac{\partial P_{\text{loss}}}{\partial \theta} \\ \frac{\partial P_{\text{loss}}}{\partial |V|} \end{bmatrix} \quad (7)$$

where P , Q , θ and $|V|$ are mismatch active and reactive power and the bus voltage phase angle and magnitude, respectively.

D. Proposed RT-SLM Algorithm

A MATLAB based algorithm has been developed to perform PEV scheduling based on RT-SLM (Fig. 2). The algorithm begins by first reading the input parameters (e.g., bus and branch impedance data, nodes with PEVs, designated priority time zones, load profiles for PEV chargers and residential loads as well as system constraints) and performing initialization (e.g., selecting the highest priority group, time zone and PEV).

The randomly arriving PEVs are added to the “PEV Queue Table” and the table is sorted from high to low priority. The queue also contains PEVs from previous time steps that have not been charged due to a constraint violation. The main program loop performs PEV coordination continuously at every time step (e.g., 5 min intervals) over 24 hours. At each time step, RT-SLM samples the current state of the smart grid (e.g., load level, loss estimates), computes MSS vector (6)–(7), sorts the “PEV Queue Table” according to MSS values, and activates PEV chargers starting from the top of the queue.

IV. SMART GRID DISTRIBUTION SYSTEM

A detailed smart grid test system topology (Fig. 4) is developed and studied to demonstrate the impacts and benefits of proposed RT-SLM versus random uncoordinated charging.

A. System Topology

The selected system is a modification of the IEEE 31 bus 23 kv distribution test system [22] combined with several residen-

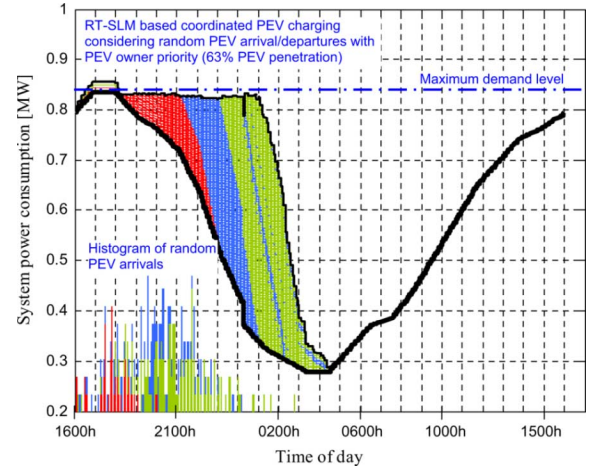


Fig. 14. Case B: Impact of MSS-based RT-SLM coordinated PEV charging (63% penetration) on the total system power demand.

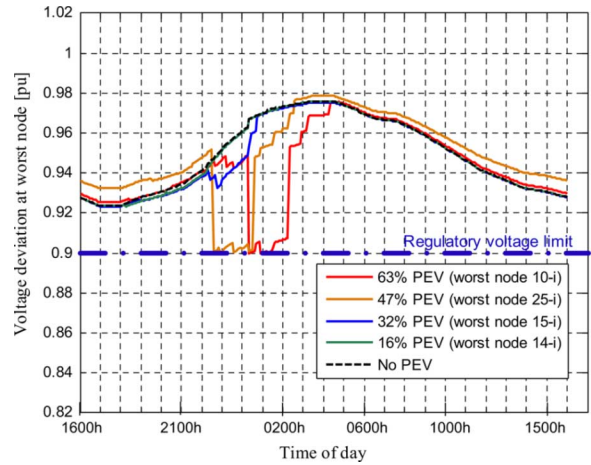


Fig. 15. Case B: Impact of MSS-based RT-SLM coordinated PEV charging on voltage profile (shown for affected worst nodes). RT-SLM maintains all voltages within regulation.

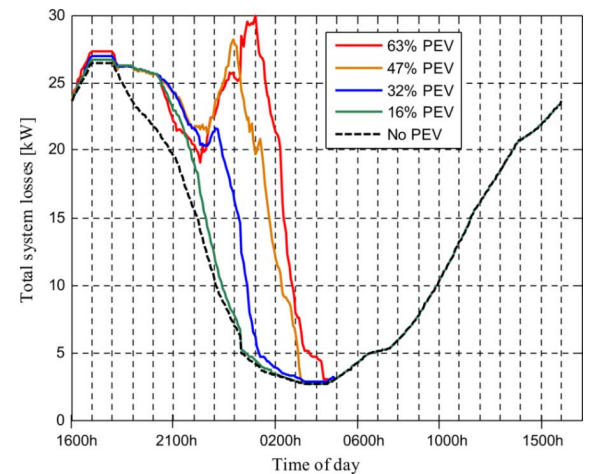


Fig. 16. Case B: Impact of MSS-based RT-SLM coordinated PEV charging on total system power losses. Note the significant reduction in losses compared to random charging.

tial LV 415 V networks based on real system data of a neighborhood (in Western Australia). Each LV feeder consists of 19 nodes representing customer households with selected nodes assigned PEVs, priority and charging zone (Table I). A total of 22 LV feeders are implemented and supplied from the HV main

buses via 23 kV/415 V 100 kVA distribution transformers. The total number of nodes is 449 (31 HV nodes and 418 LV nodes). System data are listed in the Appendix.

B. PEV Energy Requirements

For realistic modeling of PEV charging loads, the battery capacities are of importance to determine reasonable charging profiles. PEV battery capacities typically range from a few kWh to over 50 kWh [1]–[4]. For this study, a 10 kWh battery capacity per PEV is selected because it is expected that the lower end of battery sizes are more affordable and more likely to initially dominate the market.

In order to optimize PEV battery life, deep cycle batteries with a depth of discharge (DOD) of 70% of the rated battery life is assumed useable resulting in an available capacity of 7 kWh that the charger must deliver. Battery chargers have some losses and therefore the energy requirement from the grid is actually greater than the stated battery capacity. A typical battery charger efficiency of 88% is assumed [23] requiring a total of 8 kWh of energy from the grid to charge a single PEV.

C. PEV Battery Chargers

In practice, PEV battery chargers will have to be rated high enough to charge batteries of these sizes in reasonable time periods. However, limitations of household wiring must also be considered. A standard single-phase 240 V outlet (Australia) can typically supply a maximum of 2.4 kW. There are also 15A and 20A outlets (single-phase and three-phase) which can supply approximately 4 kW and 14.4 kW, respectively. For this analysis, a fixed charging power of 4 kW is selected because this is commonly available in most single-phase residential households without having to reinforce wiring.

D. Assumed Load Profiles

A typical residential load curve based on actual recordings from a distribution transformer (in Western Australia) is used to model the domestic load variations (without PEV charging) at each house over a 24 hour period (Fig. 3). The peak power consumption of a house is assumed to be on average 2 kW with a power factor of 0.9.

E. PEV Penetration Levels

In order to cover the widest range of plausible PEV charging scenarios in the near and long term future, four PEV penetration levels are simulated for each charging approach (Table I, row 2). The penetration levels are defined to be the proportion of nodes with PEVs to the total number of low voltage residential nodes (excluding transformer LV node). A maximum of one PEV per household is assumed. PEVs are randomly distributed along each low voltage network.

F. Designated PEV Priorities

Within the given penetrations, the PEVs are grouped into priority time zone groups (e.g., red, blue, and green zones, Fig. 1). A realistic breakdown of priorities is assumed by having the majority of PEVs owners subscribing to green and blue time zones.

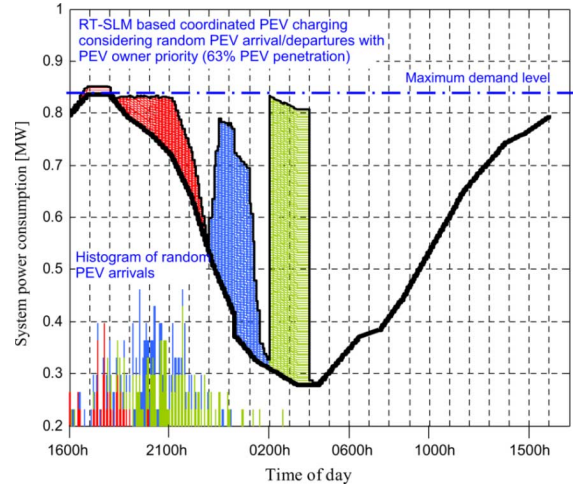


Fig. 17. Case C: Impact of MSS-based RT-SLM coordinated PEV charging (63% penetration) on the total system power demand.

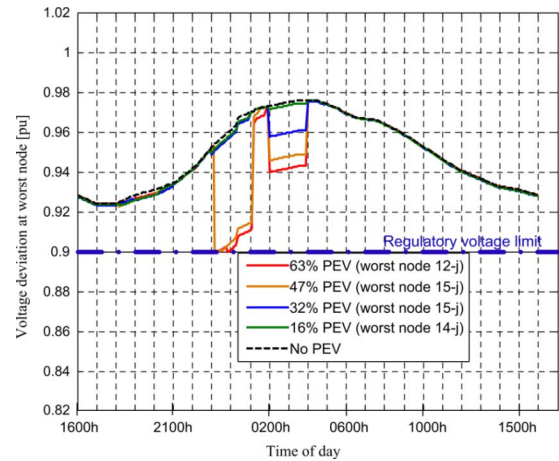


Fig. 18. Case C: Impact of MSS-based RT-SLM coordinated PEV charging on voltage profile (shown for affected worst nodes) considering PEV owner priority charging zones. RT-SLM maintains all voltages within regulation.

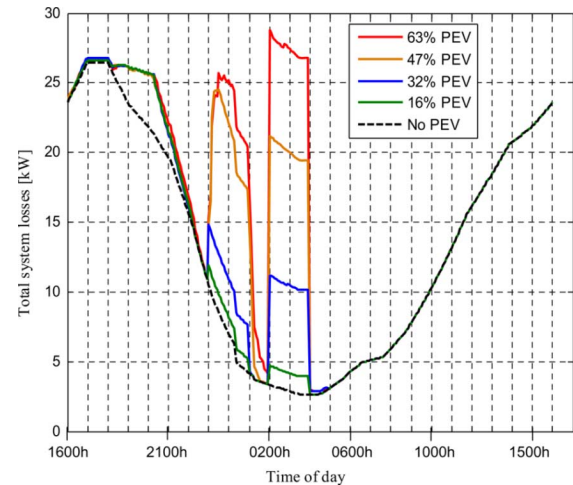


Fig. 19. Impact of MSS-based RT-SLM coordinated PEV charging on total system power losses considering PEV owner priority charging zones. Note the significant reduction in losses compared to random charging.

This is because the lower pricing of blue and green zones will be more attractive to PEV owners compared to higher tariffs in

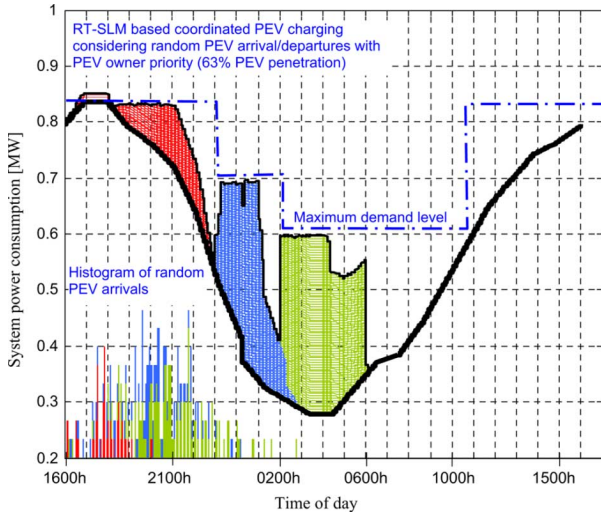


Fig. 20. Case D: Impact of MSS-based RT-SLM coordinated PEV charging (63% penetration) on the total system power demand.

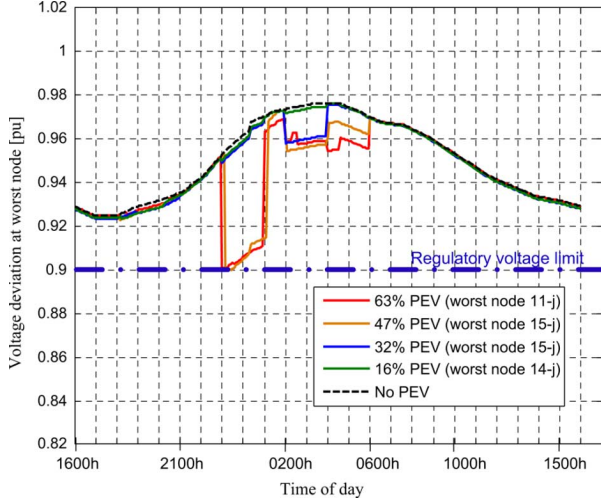


Fig. 21. Case D: Impact of MSS-based RT-SLM coordinated PEV charging on voltage profile (shown for affected worst nodes) considering PEV owner priority charging zones. RT-SLM maintains all voltages within regulation.

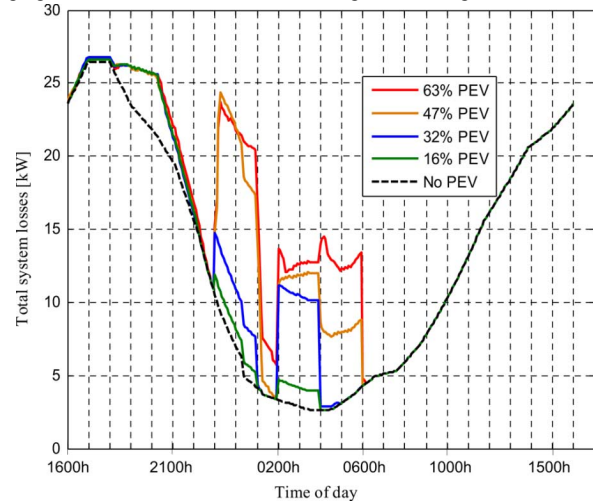


Fig. 22. Case D: Impact of MSS-based RT-SLM coordinated PEV charging on total system power losses considering PEV owner priority charging zones. Note the significant reduction in losses compared to random charging.

red zone charging. For each penetration level, the assumed priorities are randomly proportioned to the PEV nodes in each LV residential network as shown in Table I.

V. RT-SLM COORDINATION RESULTS

Simulations are performed considering four PEV charging scenarios (Table II, Cases A–D) for the smart grid system of Fig. 4. Simulation results for uncoordinated and RT-SLM coordinated PEV charging with a time step of $\Delta t = 5$ min are presented in Figs. 5–28 and Table III. The proposed algorithm of Fig. 2 is based on random arrivals of PEVs within the 24 h period. However, in order to compare simulation results of Cases B–D, a Gaussian distribution of PEV arrivals is generated and used for each penetration level as indicated by the histograms shown in Figs. 14–17, 20, and 23–28.

VI. DISCUSSION

Simulation results with PEV penetration levels of 16%, 32%, 47%, and 63% based on uncoordinated and RT-SLM coordinated charging schemes are summarized in Table III.

- Case A: Random uncoordinated PEV charging is investigated by simulating a normal distribution of PEV charging loads occurring within 1800h–0800h (Case A1, Figs. 5–7), 1800h–0100h (Case A2, Figs. 8–10), and 1800h–2200h (Case A3, Figs. 11–13). In all cases, the power demand and required generation show significant increases during the peak hours (Figs. 5, 8, and 11).
- The situation worsens for the more realistic scenario of Case A3 as the system peak rises sharply and broadens due to much of the PEV charging load coinciding with normal system load peaks. This could cause suboptimal and expensive generation dispatching with limited spinning reserve to service this new load peak. For all uncoordinated PEV charging conditions (Cases A1–A3), even with low PEV penetrations, severe voltage deviations (Figs. 6, 9, and 12), very high power losses (Figs. 7, 10, and 13), high costs in generation and energy losses (Table III, columns 5–6) are observed.
- Case B: A coordinated PEV charging strategy is proposed (Figs. 14–16, 23–25, and Table III) that considers consumer designated priorities while the three charging time zones are intentionally overlapped to begin at 1800h. It is then possible for RT-SLM to accommodate fortunate medium and low priority subscribers the opportunity to charge their vehicles earlier if after scheduling higher priority subscribers there is enough capacity without violating system constraints. In comparison with the realistic uncoordinated PEV charging scenarios (e.g., Cases A2 and A3), a general improvement in system performance and reduction in operational costs is observed (Table III). Furthermore, the voltages at all nodes are regulated within limits even under large PEV penetrations. System losses, peak generation, and transformer load currents have also reduced. However, this case may not be economically justified as some lower priority consumers are served during the red time zones at no extra charge.
- Case C: The proposed RT-SLM strategy in Case B is modified to investigate a more economically justified PEV charging strategy from the point of view of the utility (Figs. 17–19 and 26–28 and Table III). Unlike Case B, lower priority PEVs will be prevented from charging in higher priority time zones. A further reduction in

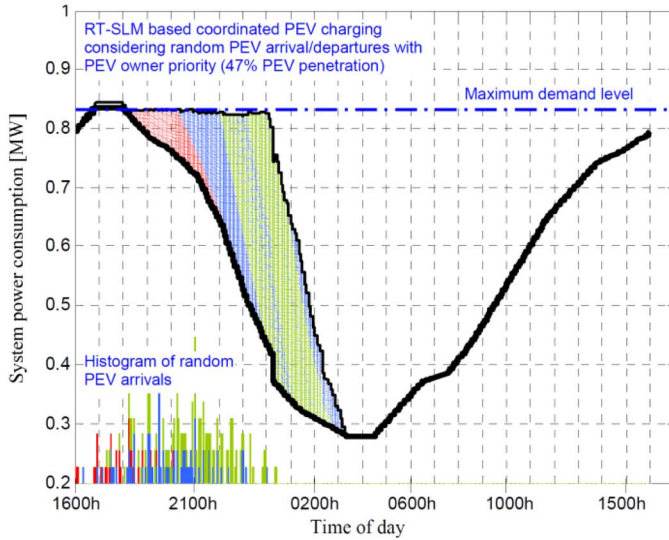


Fig. 23. Case B: System power demand with 47% penetration of PEVs using MSS-based RT-SLM coordinated PEV charging.

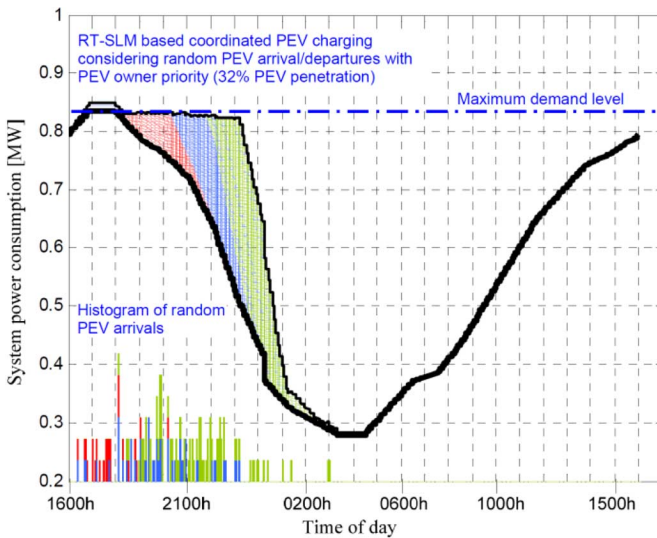


Fig. 24. Case B: System power demand with 32% penetration of PEVs using MSS-based RT-SLM coordinated PEV charging.

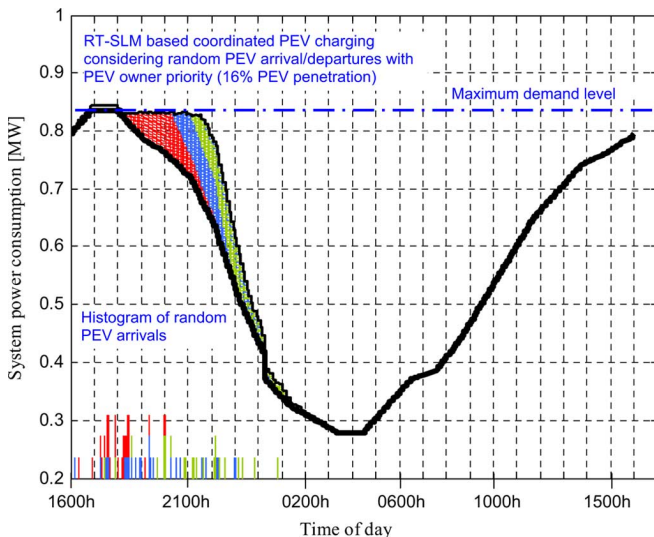


Fig. 25. Case B: System power demand with 16% penetration of PEVs using MSS-based RT-SLM coordinated PEV charging.

generation and energy loss costs is observed while maintaining similar performance improvements (e.g., voltage profile, losses, and transformer loading) of Case B. The trade-off here is that there is less customer satisfaction in not being able to charge as soon as possible given the available capacity.

- Case D: The impact of variable generation on RT-SLM performance is investigated (Figs. 20–22, and Table III). This case is representative of future smart grids where environmental factors (e.g., wind speed in wind farms) dynamically change available generation. Alternatively, utilities may wish to exercise more control in generation dispatch to achieve economic targets. Case C is modified to have step-varied demand limits. The results show the potential for further economic gains and improved smart grid performance under variable generation conditions.
- For real-time applications with large numbers of randomly arriving PEVs, RT-SLM is a good candidate for fast optimization and coordination of PEV charging in very short time steps. This is indicated by the small computing times shown for all case studies (Table III, last column). This approach has the added benefit of allowing PEVs to be charged as soon as possible while complying with network operation criteria. Furthermore, as RT-SLM utilizes a modified Newton-based load flow algorithm, it inherently has fast convergence behavior.

VII. CONCLUSION

A real-time smart load management (RT-SLM) algorithm based on MSS optimizations is proposed to improve smart grid performance with high penetration of PEVs. RT-SLM is designed for real-time coordination of randomly arriving and departing PEVs in residential networks. RT-SLM allocates PEVs for charging as soon as possible within the priority-charging time zones based on real-time (e.g., every 5 min) cost minimization while maintaining voltage profiles and generation limits. The improvements and benefits of the proposed algorithm versus uncoordinated PEV charging are compared and demonstrated through extensive simulations for a smart grid topology. The main conclusions are:

- Compared to existing PEV coordination approaches (e.g., [16]), the proposed RT-SLM is capable of real-time coordination of randomly arriving and departing PEVs considering owner charging time zone priority, direct regulation of voltage magnitudes at all nodes, controlling system peak demand while significantly improving the efficiency and economy of smart grids.
- A feasible pricing and time zone priority scheme for PEV charging is demonstrated to work effectively with SLM PEV charging coordination. PEV owners can designate preferred charging time zones as SLM performs performance improvement functions such as cost and loss minimization while maintaining voltage regulation. SLM endeavors to respect PEV owner designated charging time zones as long as system constraints are not violated.
- SLM is shown to be beneficial in reducing overall system overloads and power peaks resulting in energy savings and cost reduction through the deferment of costly upgrades and building of new generation plants. The burden on local

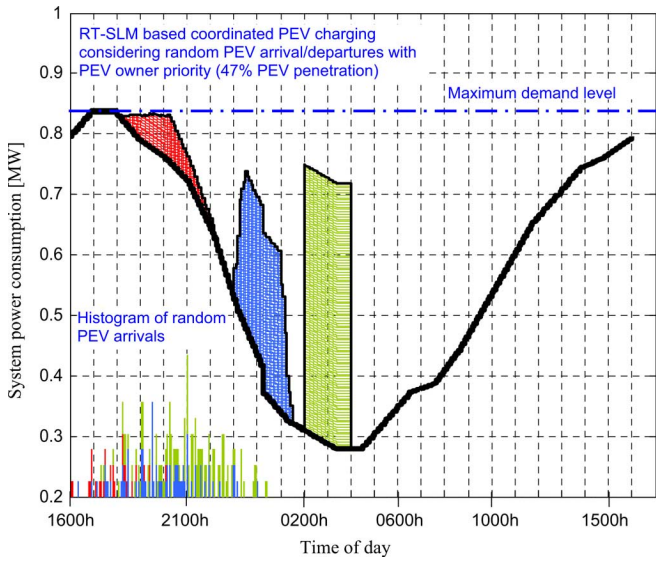


Fig. 26. Case C: System power demand with 47% penetration of PEVs using MSS-based RT-SLM coordinated PEV charging.

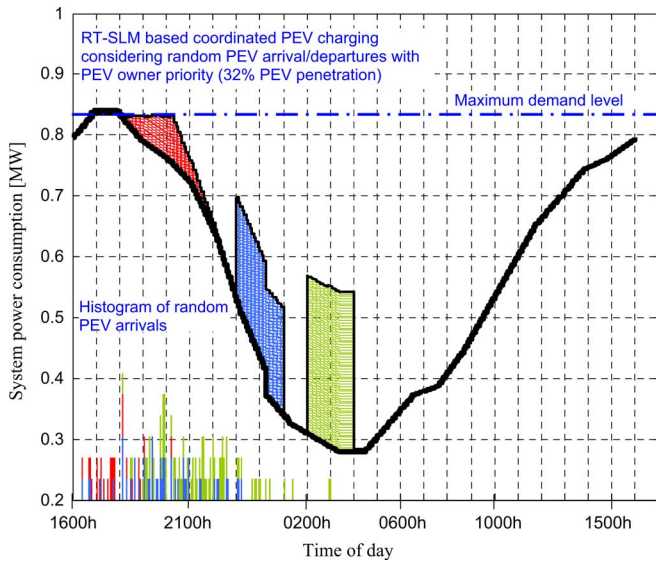


Fig. 27. Case C: System power demand with 32% penetration of PEVs using MSS-based RT-SLM coordinated PEV charging.

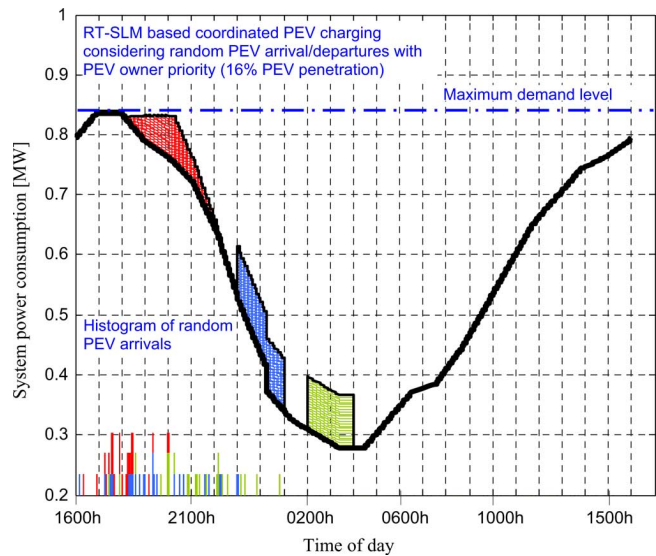


Fig. 28. Case C: System power demand with 16% penetration of PEVs using MSS-based RT-SLM coordinated PEV charging.

TABLE III
IMPACT OF UNCOORDINATED AND COORDINATED PEV CHARGING ON SMART GRID PERFORMANCE (FIG. 4) WITH RANDOMLY ARRIVING PEVS DURING THE CHARGING ZONES. FOR COMPARISON THE SAME GAUSSIAN RANDOM DISTRIBUTIONS ARE USED IN THE SIMULATIONS ($\Delta t = 5$ min)

| PEV [%] | ΔV [%] | I_{MAX} [%] | Generation cost [\$ /day] | Total cost (Eq. 3) [\$ /day] | Total cost [%]* | Computing time** [sec] |
|--|----------------|---------------|---------------------------|------------------------------|-----------------|------------------------|
| NOMINAL CASE WITHOUT ANY PEVS | | | | | | |
| 0 | 7.646 | 0.440 | 802.5 | 818.1 | 0 | 4.01 |
| Case A1 (Table II, Uncoordinated): Figs. 5-7 | | | | | | |
| 16 | 7.724 | 0.478 | 824.5 | 840.7 | 2.76 | 4.11 |
| 32 | 8.355 | 0.529 | 852.6 | 870.1 | 6.36 | 4.57 |
| 47 | 13.62 | 0.604 | 879.3 | 898.8 | 9.86 | 6.22 |
| 63 | 14.33 | 0.584 | 906.7 | 927.3 | 13.35 | 7.30 |
| CASE A2 (TABLE II, UNCOORDINATED): FIGS. 8-10 | | | | | | |
| 16 | 7.698 | 0.526 | 836.9 | 853.4 | 4.31 | 4.97 |
| 32 | 8.524 | 0.57 | 872.3 | 890.3 | 8.83 | 5.57 |
| 47 | 13.91 | 0.643 | 909.8 | 930.7 | 13.76 | 6.17 |
| 63 | 14.75 | 0.688 | 947.7 | 970.2 | 18.59 | 7.01 |
| CASE A3 (TABLE II, UNCOORDINATED): FIGS. 11-13 | | | | | | |
| 16 | 7.850 | 0.555 | 844.1 | 860.7 | 5.21 | 5.03 |
| 32 | 9.230 | 0.643 | 887.4 | 895.9 | 9.51 | 5.58 |
| 47 | 15.82 | 0.771 | 933.3 | 955.5 | 16.80 | 6.28 |
| 63 | 17.15 | 0.886 | 977.1 | 1001.5 | 22.42 | 7.20 |
| CASE B (TABLE II, COORDINATED RT-SLM): FIGS. 14-16, 23-25 | | | | | | |
| 16 | 7.657 | 0.481 | 826.8 | 843.3 | 3.08 | 10.47 |
| 32 | 7.656 | 0.482 | 859.5 | 877.2 | 7.22 | 10.46 |
| 47 | 9.999 | 0.486 | 884.4 | 904.0 | 10.50 | 10.48 |
| 63 | 10.00 | 0.515 | 905.3 | 925.8 | 13.16 | 10.74 |
| CASE C (TABLE II, COORDINATED RT-SLM): FIGS. 17-19, 26-28 | | | | | | |
| 16 | 7.657 | 0.477 | 817.1 | 833.5 | 1.88 | 10.62 |
| 32 | 7.649 | 0.477 | 838.7 | 856 | 4.63 | 10.62 |
| 47 | 9.999 | 0.478 | 860.1 | 879.4 | 7.49 | 10.69 |
| 63 | 10.00 | 0.515 | 888.3 | 908.8 | 11.09 | 10.80 |
| CASE D (TABLE II, COORDINATED RT-SLM): FIGS. 20-22 | | | | | | |
| 16 | 7.657 | 0.477 | 817.2 | 833.6 | 1.89 | 10.22 |
| 32 | 7.649 | 0.477 | 838.6 | 855.9 | 4.62 | 10.79 |
| 47 | 9.999 | 0.479 | 858.5 | 877.5 | 7.26 | 10.81 |
| 63 | 9.999 | 0.515 | 884.3 | 904.1 | 10.51 | 11.01 |

*) Increase in total cost as a percentage of nominal cost with no PEVs.

***) Intel Core 2 Quad 3.0 GHz processor, 8 GB RAM, using MatLab ver. 7.

distribution circuits is also reduced (e.g., cables and transformers) thereby minimizing the risk and cost of premature transformer failures and associated outages.

- Conventional optimization approaches (e.g., GAs) are generally too computationally intensive to be of any practical use for real-time PEV coordination. Therefore, the high speed performance offered by RT-SLM with MSS optimization could be a viable option to cope with the frequent and random nature of PEV charging activities.
- The impact of PEV charging was the focus of this study; however, the SLM approaches are applicable to coordinating a wider range of smart appliances.
- The results obtained through the SLM approach are vital for smart grid reinforcement by improving the reliability and security of the supply to the customer.

APPENDIX

Parameters of the 19 bus low voltage and 31 bus distribution system are provided in Tables IV–V [22], respectively.

TABLE IV
LINEAR AND NONLINEAR (PEV) LOADS OF THE TYPICAL LOW VOLTAGE RESIDENTIAL SYSTEM (FIG. 4)

| Linear and PEV Load | | Power | |
|---------------------|--------------|-------|------|
| Bus | Name | kW | kVAR |
| 1 to 19 | Linear loads | 2.0 | 0.97 |
| Selected buses | PEV charger | 4.0 | 0 |

TABLE V
LINE PARAMETERS OF THE LOW VOLTAGE RESIDENTIAL SYSTEM (FIG. 4)

| LINE | | Line resistance R [Ω] | Line reactance X [Ω] | LINE | | Line resistance R [Ω] | Line reactance X [Ω] |
|----------|--------|--------------------------------|-------------------------------|------------------------------------|--------|--------------------------------|-------------------------------|
| From bus | To bus | | | From bus | To bus | | |
| a | b | 0.0415 | 0.0145 | f | l | 1.3605 | 0.1357 |
| b | c | 0.0424 | 0.0189 | d | m | 0.140 | 0.0140 |
| c | d | 0.0444 | 0.0198 | c | n | 0.7763 | 0.0774 |
| d | e | 0.0369 | 0.0165 | b | o | 0.5977 | 0.0596 |
| e | f | 0.0520 | 0.0232 | a | p | 0.1423 | 0.0496 |
| f | g | 0.0524 | 0.0234 | p | q | 0.0837 | 0.0292 |
| g | h | 0.0005 | 0.0002 | q | r | 0.3123 | 0.0311 |
| g | i | 0.2002 | 0.0199 | a | s | 0.0163 | 0.0062 |
| g | j | 1.7340 | 0.1729 | Distribution transformer reactance | | 0.0654 | |
| f | k | 0.2607 | 0.0260 | | | | |

REFERENCES

- [1] Tesla Motors—High Performance Electric Vehicles 2010 [Online]. Available: <http://www.teslamotors.com>
- [2] Nissan LEAF Electric Car 2010 [Online]. Available: <http://www.nissansusa.com/leaf-electric-car>
- [3] Chevrolet, 2011 Volt Electric Car 2010 [Online]. Available: <http://www.chevrolet.com/electriccar>
- [4] A. S. Masoum, S. Deilami, P. S. Moses, M. A. S. Masoum, and A. Abu-Siada, "Smart load management of plug-in electric vehicles in distribution and residential networks with charging stations for peak shaving and loss minimization considering voltage regulation," *IET Proc. Gener., Transm., Distrib.*, vol. 5, no. 8, pp. 877–888, 2011.
- [5] T. Gönen, *Electric Power Distribution System Engineering*. Boca Raton, FL: Taylor & Francis, 2007.
- [6] S. M. Amin and B. F. Wollenberg, "Toward a smart grid: Power delivery for the 21st century," *IEEE Power Energy Mag.*, vol. 3, no. 5, pp. 34–41, 2005.
- [7] S. M. Amin, "For the good of the grid," *IEEE Power Energy Mag.*, vol. 6, no. 6, pp. 48–59, 2008.
- [8] E. M. Lightner and S. E. Widergren, "An orderly transition to a transformed electricity system," *IEEE Trans. Smart Grid*, vol. 1, no. 1, pp. 3–10, Jun. 2010.
- [9] Q. B. Dam, S. Mohagheghi, and J. Stoupis, "Intelligent demand response scheme for customer side load management," in *Proc. IEEE Energy 2030 Conf.*, 2008, pp. 1–7.
- [10] G. Mauri, D. Moneta, and C. Bettoni, "Energy conservation and smart-grids: New challenge for multimetering infrastructures," in *Proc. IEEE Bucharest PowerTech*, 2009, pp. 1–7.
- [11] A. Chuang and C. Gellings, "Demand-side integration for customer choice through variable service subscription," in *Proc. IEEE Power Energy Soc. Gen. Meet.*, 2009, pp. 1–7.
- [12] S. Bruno, S. Lamonaca, M. L. Scala, G. Rotondo, and U. Stecchi, "Load control through smart-metering on distribution networks," in *Proc. IEEE Bucharest PowerTech*, 2009, pp. 1–8.
- [13] F. Rahimi and A. Ipakchi, "Demand response as a market resource under the smart grid paradigm," *IEEE Trans. Smart Grid*, vol. 1, no. 1, pp. 82–88, Jun. 2010.
- [14] F. Jiyuan and S. Borlase, "The evolution of distribution," *IEEE Power Energy Mag.*, vol. 7, no. 2, pp. 63–68, 2009.
- [15] A. Ipakchi and F. Albuyeh, "Grid of the future," *IEEE Power Energy Mag.*, vol. 7, no. 2, pp. 52–62, 2009.
- [16] K. Clement-Nyns, E. Haesen, and J. Driesen, "The impact of charging plug-in hybrid electric vehicles on a residential distribution grid," *IEEE Trans. Power Syst.*, vol. 25, no. 1, pp. 371–380, 2010.
- [17] K. Moslehi and R. Kumar, "A reliability perspective of the smart grid," *IEEE Trans. Smart Grid*, vol. 1, no. 1, pp. 57–64, Jun. 2010.
- [18] B. D. Russell and C. L. Benner, "Intelligent systems for improved reliability and failure diagnosis in distribution systems," *IEEE Trans. Smart Grid*, vol. 1, no. 1, pp. 48–56, Jun. 2010.
- [19] A. R. Metke and R. L. Ekl, "Security technology for smart grid networks," *IEEE Trans. Smart Grid*, vol. 1, no. 1, pp. 99–107, Jun. 2010.
- [20] P. Jeongje, C. Jaeseok, M. Shahidehpour, K. Y. Lee, and R. Billinton, "New efficient reserve rate index of power system including renewable energy generators," in *Proc. Int. Conf. Innov. Smart Grid Technol. (ISGT)*, 2010, pp. 1–6.
- [21] C. Jaeseok, P. Jeongje, M. Shahidehpour, and R. Billinton, "Assessment of CO₂ reduction by renewable energy generators," in *Proc. Int. Conf. Innov. Smart Grid Technol. (ISGT)*, 2010, pp. 1–5.
- [22] S. Civanlar and J. J. Grainger, "Volt/var control on distribution systems with lateral branches using shunt capacitors and voltage regulators part III: The numerical results," *IEEE Trans. Power App. Syst.*, vol. PAS-104, no. 11, pp. 3291–3297, 1985.
- [23] M. Duvall, E. Knipping, and M. Alexander, "Environmental assessment of plug-in hybrid electric vehicles," *EPRI: Nationwide Greenhouse Gas Emissions*, vol. 1, 2007.
- [24] S. Han, S. Han, and K. Sezaki, "Development of an optimal vehicle-to-grid aggregator for frequency regulation," *IEEE Trans. Smart Grid*, vol. 1, no. 1, pp. 65–72, Jun. 2010.
- [25] E. Sortomme and M. A. El-Sharkawi, "Optimal charging strategies for unidirectional vehicle-to-grid," *IEEE Trans. Smart Grid*, vol. 2, no. 1, pp. 131–138, Mar. 2011.
- [26] J. R. Pillai and B. Bak-Jensen, "Integration of vehicle-to-grid in the Western Danish power system," *IEEE Trans. Sustainable Energy*, vol. 2, no. 1, pp. 12–19, 2011.
- [27] M. A. S. Masoum, M. Ladjevardi, E. F. Fuchs, and W. Grady, "Application of local variations and maximum sensitivities selections for optimal placement of shunt capacitor banks under nonsinusoidal operating conditions," *Int. J. Electr. Power Energy Syst.*, vol. 26, no. 10, pp. 761–769, 2004.
- [28] M. A. S. Masoum, M. Ladjevardi, E. F. Fuchs, and W. Grady, "Optimal sizing and placement of fixed and switched capacitor banks under nonsinusoidal operating conditions," in *Proc. IEEE PES-2002 Summer Meet.*, Chicago, IL, Jul. 2002, pp. 807–813.
- [29] M. A. S. Masoum, M. Ladjevardi, A. Jafarian, and E. F. Fuchs, "Optimal placement, replacement and sizing of capacitor banks in distorted distribution networks by genetic algorithms," *IEEE Trans. Power Del.*, vol. 19, no. 4, pp. 1794–1801, Oct. 2004.
- [30] P. Wolfs, "An economic assessment of second use lithium ion batteries for grid support," in *Proc. Australas. Univ. Power Eng. Conf. (AUPEC)*, 2010.



Sara Deilami (S'09) received the B.S. degree in electrical engineering from Islamic Azad University, Tehran, Iran, in 2000 and the M.S. degree in electrical engineering from Curtin University, Perth, WA, Australia in 2011. She is currently working toward the Ph.D. degree in electrical engineering at Curtin University.

She was awarded a Curtin University Postgraduate Scholarship (CUPS) and an Australian Postgraduate Award (APA) scholarship in 2010 and 2011, respectively. She has nine years of industry experience as

an engineer working in consultant companies.



Amir S. Masoum (S'09) received the B.S. and M.S. degrees in electrical engineering and electrical utility engineering from the University of Western Australia, WA, Australia, and Curtin University, Perth, WA, Australia in 2009 and 2010, respectively. He is currently working toward the Ph.D. degree in electrical engineering at Curtin University, Australia.

He has been a Project Manager at the Operational Asset Management, Western Power, Kewdale, WA, since 2010. His research interests include optimization, control and management of smart grid, distributed generation, and renewable energy systems.



Paul S. Moses (S'09) received the B.Eng. (1st Class Hons.) and B.S. degrees in electrical engineering and physics from Curtin University, Perth, Australia, in 2006. He is presently working towards a Ph.D. degree in Electrical Engineering at Curtin University.

Since 2007, he has worked as a Research Scientist for the Defence Science and Technology Organisation (DSTO), Department of Defence, HMAS Stirling, Australia, and is presently part of their Maritime Platforms Division, Propulsion and Energy Systems Group. His research interests include nonlinear elec-

tromagnetic phenomena, power quality and protection. He was awarded an Australian Postgraduate Award scholarship in 2009.



Mohammad A.S. Masoum (S'88-M'91-SM'05) received the B.S., M.S., and Ph.D. degrees in electrical and computer engineering, from the University of Colorado, Boulder, in 1983, 1985, and 1991, respectively.

Currently, he is an Associate Professor and the Discipline Leader for Power System Engineering at the Electrical and Computer Engineering Department, Curtin University, Perth, Australia. He is the coauthor of *Power Quality in Power Systems and Electrical Machines* (Elsevier, 2008) and *Power*

Conversion of Renewable Energy Systems (Springer, 2011).